

# Water flow impedance through a fracture made by hydraulic pressure

Hideo KOBAYASHI, Yasuki OIKAWA, Isao MATSUNAGA

National Institute for Resources and Environment  
Onogawa 16-3, Tsukuba, Ibaraki, 305 JAPAN

Key words - flow impedance, hydraulic fracture, fracture aperture, Hot Dry Rock

## Abstract

The objectives of these studies are to collect basic data on the deformation of rock samples during the extension of a hydraulic fracture and on the fracture deformation during injection of water into a fracture. Inada granite was used for the tests. The deformation of the rock samples were measured by several LVDTs and pai-gauges in order to estimate initial fracture width and the mean aperture of hydraulic fractures. The Rock deformations during the hydraulic fracturing considered to be equal to the fracture aperture were about  $20910^{-6}\text{m}$  independent whether the fractures were created parallel to the rift plane or parallel to the hardway plane. During cyclic loading of the fractures the amplitude of fracture displacement decreased and flow impedance in the fracture increased.

## 1. Introduction

Hydraulic fracturing and well stimulations are commonly used to improve productivity and injectivity of geothermal wells and to create an artificial reservoirs for heat extraction from hot dry rock formations. The characterization of fluid flow through fractures is very important as the hydraulic properties of the crystalline rock is determined predominantly by the hydraulic properties of the fractures contained in the rock mass.

At Hijiori HDR test site a circulation system was established in the granodiorite below 1,500m. Many stimulation and injection tests were performed in order to determine the hydraulic characteristics of the artificial reservoir. It was observed that the injection pressure decreased in the course of these tests extending over a time period of several years (Oikawa 1992). This means that flow impedance of fractures composing the reservoir decreased due to the cyclic water injection. It might be suspected that self propping of the fractures during the injection tests affected this decrease of the flow impedance. The data obtained during the field tests are related to the total flow impedance of the reservoir. They do not yield information on individual fractures.

Raven(1985) reported that water flow rate in a natural fracture was found to decrease with each additional loading cycle on the fracture. In order to investigate the flow impedance in hydraulically made single fractures, laboratory tests were performed on rock samples containing a hydraulically induced fracture. Inada granite was used for the test. The injection pressure and the deformation of the rock sample supposed to be equal to the mean aperture of the fracture were measured during injection at a constant flow rate for cyclic loading of the fracture. The surface of the hydraulically induced fractures contacted partially and the water flowed through connected channels within the fracture plane.

## 2. Experimental Procedures

Rock samples from Inada granite obtained from a quarry in Inada town, Ibaraki were used. The granite is coarse grained with sizes ranging from 0.2mm to 2mm and quartz grains up to 4mm.

It is well known that the Inada granite rock mass behaves as a anisotropic material. The uniaxial tensile strengths perpendicular to rift plane and hardway plane are 4.2MPa and 7.05MPa respectively. The permeability of the Inada granite along the rift plane at atmospheric condition is  $3.8 \times 10^{-9}\text{cm/sec}$  (Kosugi, 1987).

A small hole of 10mm in diameter was drilled at the center of a 200mm cubic block of Inada granite to make a hydraulic fracture with a mechanical type packer of silicon rubber. The length of the pressurized zone ranged between 30 to 50mm, and injection flow rate during fracturing ranged between 6 to 12  $\text{cm}^3/\text{min}$ . As mentioned above, the Inada granite has a mechanical anisotropy therefore fractures created hydraulically in different orientations with respect to its anisotropy may show different behaviors under normal stress acting to the fracture plane and water flow through the fracture. To examine the influence of its anisotropy on the fracture behaviors, we carried out three types of hydraulic fracturing tests as follows.

- a) with a hole parallel to the rift plan under atmospheric stress
- b) with a hole perpendicular to the rift plane under 2-axial compressive stress to the hole axis
- c) with a hole perpendicular to the hardway plane under 2-axial compressive stress to the hole axis

In cases b) and c), 8-10MPa compressive stresses to the cubic rock sample were applied by oil pressure supplied to flat jacks. Fractures created in cases a) and b) were parallel to rift plan, and fractures created in case c) were parallel to the hardway plan. Flow rate, injection pressure and deformation of the rock blocks resulting from the occurrence of the hydraulic fracture were measured during hydraulic fracturing. Fig.1 shows a test block for the hydraulic fracturing test in case a). One radar displacement meter, O, 4 LVDTs: A,B,C,D are situated on the upper surface of the test block and 2 pai-gauges, E,F are affixed at the side wall of the block where the hydraulic fracture was expected to reach the surface. The data sampling interval for the hydraulic fracturing tests and the flow impedance tests were 50msec and 0.2sec respectively.

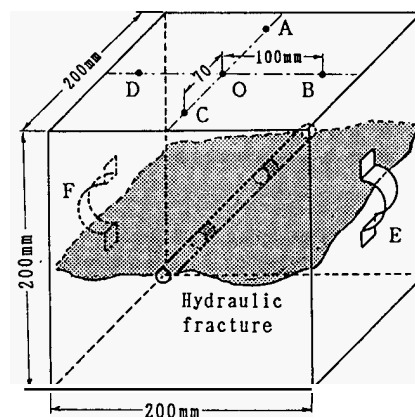


Fig.1 Scheme of a rock block for the hydraulic fracturing test

In case b) and c), fractures were created perpendicular to the hole axis, and only two sets of LVDTs affixed to two opposite surface of the block were monitored. After extending the fracture to the side walls of the rock block, an overcoring core was collected which diameter was 150mm and height was 200mm, for the flow impedance tests. During the overcoring the fracture plane did not separated which told us that some part of the fracture plane was still connected.

Flow tests here conducted under uniaxial stress conditions. Before the tests, water injection to the hydraulic fracture was continued for about 1 hour to permeate sufficient water into the vicinity of the fracture plane and around the injection hole of the test specimen to maintain stable conditions of water saturation for the flow tests. During the tests, flow rate, injection pressure, uniaxial stress and the longitudinal deformation of the test core at two different positions on the wall of the core were monitored. Figure 2 is a scheme of a sample placed within the loading frame for flow testing. The fracture deformation due to fluid pressure and uniaxial stress was given by subtracting the rock deformation detected at an intact part by 3 pai-gauges from the deformation measured by 4 pai-gauges across the fracture.

After finishing the flow impedance tests, the fracture deformation under uniaxial stress condition was measured without water injection to the fracture.

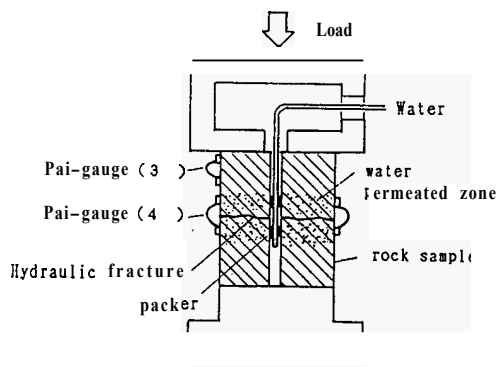


Figure 2 Scheme of a rock sample placed within the loading frame for testing

### 3. Experimental results

#### 1) Deformation of the rock samples during hydraulic fracturing tests

Figure 3 shows an example of the injection pressure and the deformations of a rock block detected by two pai-gauges: E and F during a hydraulic fracturing test of case a). The injection pressure rose to about 14MPa when the fracture was initiated and was held stable at about 4 Mpa in the following cyclic injection. The deformation of the rock wall, caused by the creation of the hydraulic fracture increased with the cyclic fluid injection and reached a stable value at the end. In this case, the aperture of the fracture detected at both side of the rock block where a hydraulic fracture reached the side walls were  $18 \times 10^{-6} \text{m}$  and  $32 \times 10^{-6} \text{m}$ . For fractures created parallel to the rift plane the aperture detected at the side walls were  $20\text{--}30 \times 10^{-6} \text{m}$ , and these values decreased by about  $5 \times 10^{-6} \text{m}$  after drying the sample.

The data sampling interval during the hydraulic fracturing tests was rather short (50msec). We checked the time difference between  $P_{\text{max}}$  (breakdown pressure) and the start time of rock deformation (fracture initiation). Fig 4 is an example of the records of water pressure and rock deformation when the hydraulic fracture was initiated parallel to the rift plane as shown in Fig 1. The injection pressure reached the maximum value at time 1.5sec in this Fig, whereas the displacements

started a little bit later. In this case, displacement at O, at B and D, at E and F started 0.3sec, 0.4–0.7sec, 0.8–0.9sec later than the time of maximum injection pressure.

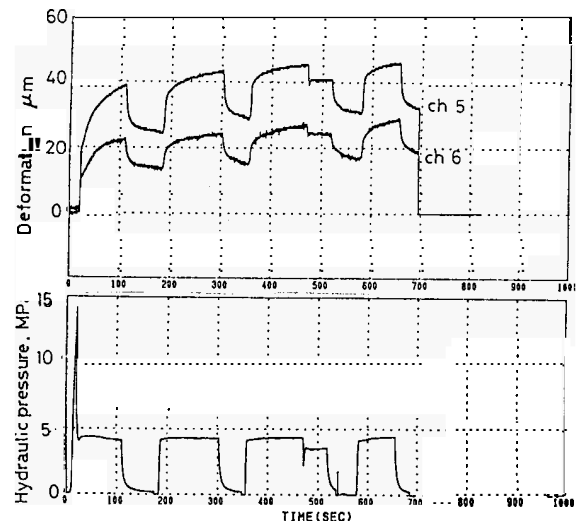


Fig 3 Deformation and hydraulic pressure recorded during the extension of a hydraulic fracture (ch5: E, ch6 F)

8 rock blocks were hydraulically fractured to determine the time difference between  $P_{\text{max}}$  time and the start of deformation at several point of the block at different distances from the injection point. The time differences were as follows.

- at point O: 0.21sec
- at point B and E: 0.35sec
- at Point E and D: 0.48sec

We have not collected sufficient data on the time difference between  $P_{\text{max}}$  and the start of deformation at different points on the rock block to evaluate the speed of fracture extension. But it is expected to estimate roughly the speed of fracture extension (Kobayashi, 1994).

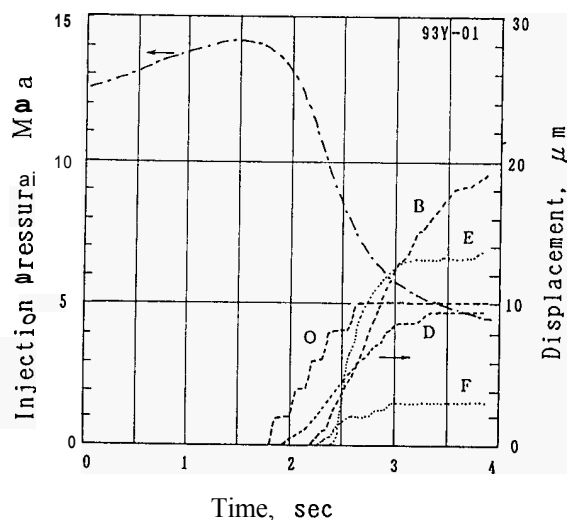


Figure 4 Time difference between the maximum value of injection pressure and start of rock deformations (O, at the center point on the upper surface of the block) (B, D at points 75mm apart from point O) (E, F at the sidewall of the block, 100mm apart from the injection point)

#### 2) Flow tests through the hydraulic fractures

Before the flow tests, water injection, at constant flow rate of  $6 \text{cm}^3/\text{min}$ , to the hydraulic fracture was continued to permeate

sufficient water into the vicinity of the fracture plane, therefore, the fracture was open to a certain value when normal load was applied. Then we applied the normal stress to the fracture. With the increase of the normal stress to the fracture, the injection pressure increased due to the closer of the fracture (the deformation of the fracture). During the flow tests, the maximum injection pressure was maintained under about 8MPa to restrict the initiation of a new hydraulic fracture along the injection hole of the specimen. Fig.5 shows the deformation of a fracture created in the rift plane (IG06R) during the up-loading period of each loading cycle. The deformation of the fracture decreased with the number of loading cycles. The fractures created in the hardway plane showed the same trend.

The flow rate per pressure unit decreased with the increase of the normal stress on the fracture and with the number of loading cycles (Fig.6). This corresponds with the decrease of the mean aperture of the fracture with the number of loading cycles as shown in Fig.5. The flow rate per pressure unit through the fracture in the hardway plane is less than that of in the rift plane, whereas mean apertures of both type fractures were almost the same ( $20 \times 10^{-6} \text{m}$ ). The difference of the injection pressures for the two cases may be caused by the different roughness of the two type of fractures. Gale(1987) pointed out that the contact area between the walls of the hydraulic fracture is a function of the surface roughness of the fracture. Therefore the surface roughness has to be determined for further investigations on the characteristics of hydraulic fractures.

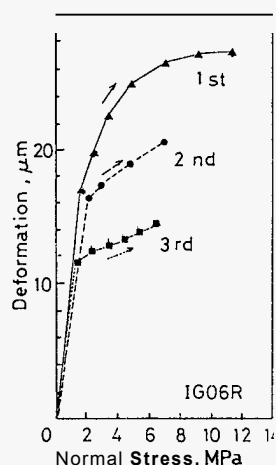


Fig 5 Deformation of the hydraulic fracture as a function of the normal stress at a constant injection rate of  $6 \text{cm}^3/\text{min}$  (IG06R)

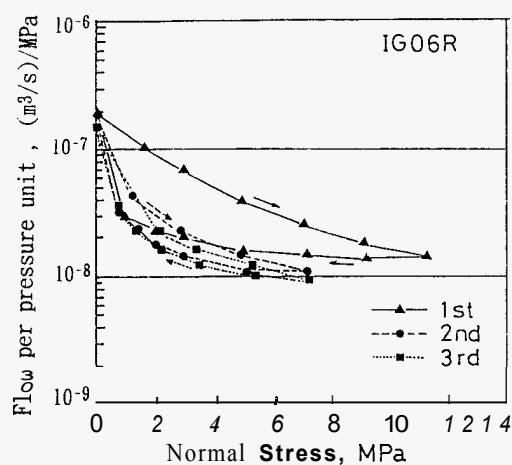


Fig 6 Fracture flow rate per pressure unit as a function of the normal stress (IG06R)

From the fracture flow impedance, an equivalent aperture (parallel plate model) was estimated assuming that the cubic law could be applied to the flow in hydraulic fractures.

The cubic law is written as

$$Q/\Delta H = C(2b)^3 \quad (1)$$

Where  $Q/\Delta H$  = Flow rate per unit pressure through fracture,  
 $2b$  = effective fracture aperture,  
 $C$  = constant which in the case of radial flow is given by,

$$C = (2\pi\rho g)/12\mu\ln(r_e/r_w) \quad (2)$$

Where  $\rho$  = fluid density,  $g$  = acceleration of gravity,  
 $\mu$  = dynamic viscosity of fluid,  
 $r_e$  = outer radius,  $r_w$  = well bore radius

Equivalent hydraulic aperture of the fracture in rift plane and hardway plane are  $12 \times 10^{-6} \text{m}$  and  $6 \times 10^{-6} \text{m}$  respectively, which is less than the detected aperture, of about  $20 \times 10^{-6} \text{m}$ , for both cases of fractures. The difference of the equivalent values for the two cases may be caused by the different roughness and channeling of the two types of fractures.

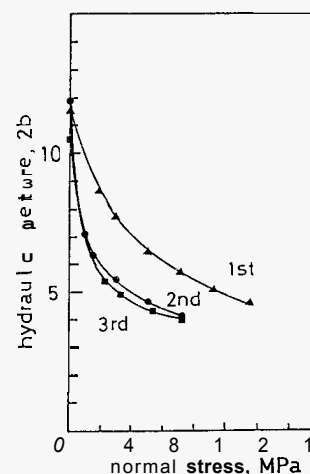


Fig 7 Hydraulic aperture of a fracture in the rift plane as a function of normal stress (IR06R)

### 3) Displacement of a hydraulic fracture as a function of the normal stress on the fracture plane

After finishing the flow tests under constant flow rate and cyclic loading, fracture displacement was examined under cyclic loading without water injection. Fig.8 and Fig.9 show the displacement of normal stress. The displacements of intact rock and across the fracture showed the same behavior when the normal stress exceeded several MPa for both cases, which tell us that stiffness of a hydraulic fracture in granite is almost same as that of intact rock when normal stress to the fracture is over several MPa.

### 4. Water injection tests into an artificial reservoir created in the Hijiori hot dry rock test site

An artificial geothermal reservoir has been created hydraulically at the Hijiori hot dry rock test site. Many injection and stimulation tests were carried out to evaluate the characteristics of the reservoir. The well SKG-2 drilled to a depth of 1,802m was used for these tests. A 7" casing is installed all along the well down to a depth of 1,788m leaving 14m open hole section at the bottom. Water is injected into the crystalline granodiorite basement rock, from this open hole section. During each injection test, flow rate and injection pressures at the well head were measured, and in some cases pressures in the bottom hole were monitored by a PTS (pressure, temperature, spinner) logging tool.

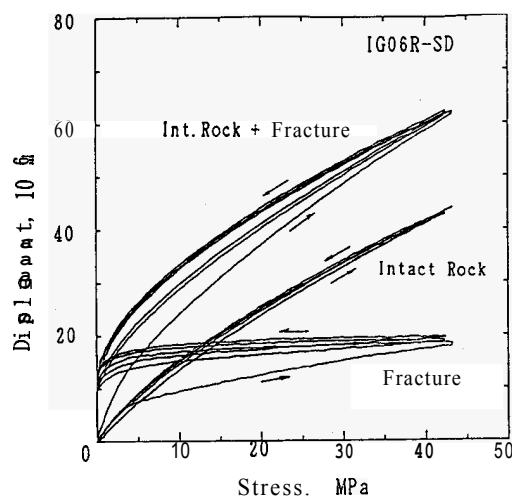


Fig 8 Fracture and rock displacement as a function of normal stress without water injection (IG06R-SD: fracture is created in the rift plane)

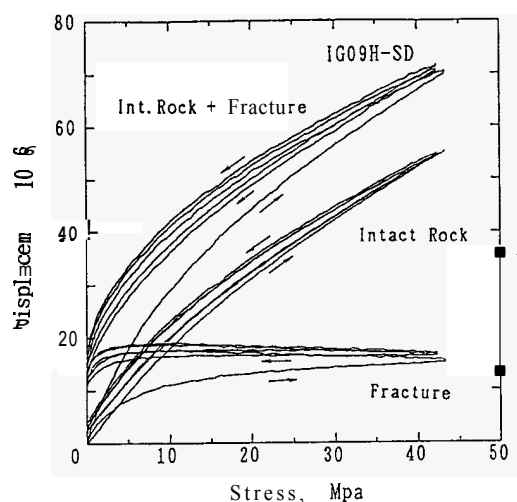


Fig 9 Fracture and rock displacement as a function of normal stress without water injection (IG09H-SD: fracture is created in the hardway plane)

Fig. 10 shows a present schematic view of wellbores from 1,500m to 1,900m. In 1985, the test site was located at the rim of the Hijiori caldera and first injection test was conducted. Many times of hydraulic fracturing, stimulation and injection tests were conducted periodically as follows,

- 1985 a small scale injection test with SKG-2 well
- 1986 1,800m deep reservoir was stimulated with SKG-2 well
- 1987 drill HDR-1 well to the reservoir, injection tests
- 1988 15 days circulation test between SKG-2 and HDR-1 including massive stimulation and injection tests
- 1989 drill HDR-2 well to the reservoir, injection tests 29 days circulation test with SKG-2 and two production wells (HDR-1, HDR-2) including massive stimulation
- 1990 drill HDR-3 well to the reservoir and injection tests
- 1991 90 days circulation tests and injection tests

To evaluate the flow characteristics of the artificial reservoir, the bottom hole pressure were calculated by numerical simulation (WBHT: Wellbore Heat Transfer Cord, Smith et al, 1982) using flow rates and wellhead pressures of each experiment.

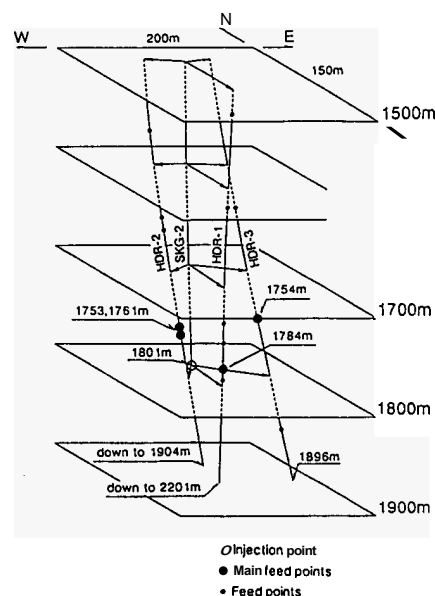


Fig 10 Schematic view of wellbores (Yamaguchi, 1992)

Fig 11 shows the relationship between the estimated stable pressure at the bottomhole and the flow rate during the years 1985 to 1990. It is obvious that the bottomhole pressure required to inject at a certain flow rate decreased gradually during the injection sequence.

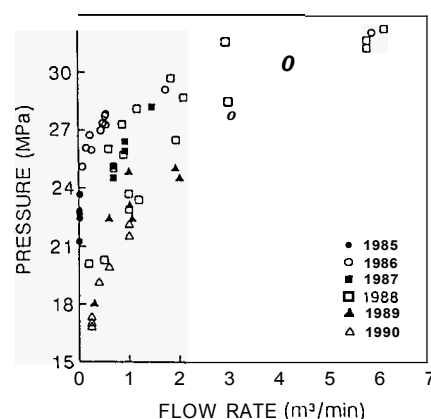


Fig 11 Relationship between bottom hole pressures and the flow rate during the years 1985 to 1991

The permeability of rock around the open hole section was calculated with assumption of radial flow in a disk of height: 14m, radius: 500m (based on distribution of AE during stimulation). Fig.12 shows relationship between the rock permeability and the differential pressure ( pressure difference at bottom hole caused by water injection ) All the experiments were divided into four term, i.e. term 1 (Exp.8501-8603), Term 2 (Exp.8604-8801), term 3 (Exp.8802-8901) and term 4 Exp 8902-9004). The first experiment of each term is latter big stimulation. In each term, the permeability was not constant but increased with the increase of the bottom hole pressure. The permeability at certain differential pressure increased significantly after hydraulic stimulation tests, such as Exp.8604, Exp 8802 and Exp 8902 in which a large amount of water compared to the former experiments was injected under high pressure. It may be considered that new fractures might be created in the rock around the open hole section of the injection well during such hydraulic stimulation tests

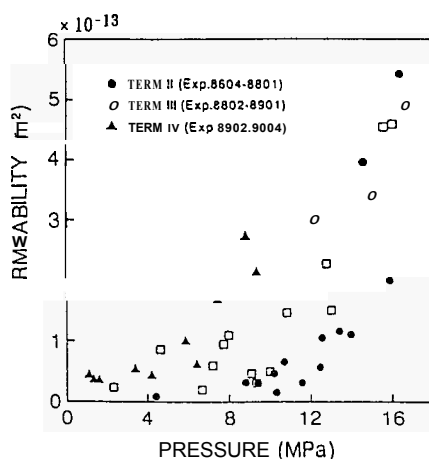


Fig 12 Relationship between permeability and differential pressure after the massive hydraulic fracturing ,Exp 8604

## 5. Conclusions

1) The deformation of Inada granite blocks caused by creating a hydraulic fracture is about  $20 \times 10^{-6} \text{m}$  for both fractures in rift plane and hardway plane. This value is regarded as the initial aperture of a hydraulic fracture in this study

2) The injectivity at constant injection rate decreased with the numbers of loading cycles. This corresponds to an increase of the flow impedance in the fracture.

3) The bottom hole pressure required to inject water at a certain flow rate at the Hijiori HDR field decreased during repeated injection. That is in contrary to the trend observed during the laboratory tests.

## Acknowledgments

The authors would like to acknowledge the assistance provided in the laboratory by Mr. Yamamoto, H., Mr. Taguchi, H. and Mr. Dewa, M. Tokai university

## References

- Gale, G.E. (1987). Comparison of coupled fracture deformation and fluid flow in rocks with deformable measurements of fracture pore structure and stress-flow properties, Proc. 28th US Symp. on Rock Mech. Tucson, pp.1213-22
- Kobayashi, H. and Oikawa, Y., and Yamamoto, H. (1994) Displacement and flow impedance of a fracture created hydraulically. Proce Annual. Meeting of Mining and Materials Processing Institute of Japan,
- Kosugi, M., Kobayashi, H. and Hayamizu, H. (1987). Studies on the Mechanism of hydraulic fracturing in Anisotropic Rocks, Report of Nat. Res. Inst. for Pollution and Resources, No.43,
- Oikawa, Y., Matsunaga, I., Yamaguchi, T., Sato, Y., Kuriyagawa, M. and Kobayashi, H. (1992). Bottomhole Pressure Behavior in the Injection well at Hijiori HDR site. J. Geoth. Res. Soc. Japan, Vol.14 No.3, PP. 273-289
- Raven, K.G. and Gale, J.E. (1985) Water Flow in a Natural Rock Fracture as a function of stress and sample size Int. J. Rock Mech. Min. Sci. & Geomech. Abstr. Vol.22, No.4, PP 251-261
- Smith, M.C., Nunz, G.J. and Ponder, G.M., (1982). Hot Dry Rock Geothermal energy Development Program, LA-9780-HDR
- Yamaguchi, T., Hiwaki, N., Abe, T. and Oikawa, Y. (1992) 90-day circulation test at Hijiori HDR test site, Geothermal Resources Council Transactions, Vol. 16, Oct. 1992